PRELIMINARY ANALYSIS OF RED MUD SPILL BASED ON AERIAL IMAGERY

PÉTER BURAI[1,2] – AMER SMAILBEGOVIC[3] – CSABA LÉNÁRT[4] – JÓZSEF BERKE[5] – GÁBOR MILICS[6] – TAMÁS TOMOR[7] – TIBOR BÍRÓ[8]

[1]Károly Róbert College, Faculty of Natural Resources Management and Rural Development, Institute of Agroinformatics and Rural Development, H-3500 Gyöngyös Mátrai út 36., Hungary, E-mail: pburai@karolyrobert.hu; [2]Envirosense Hungary, H-4028 Debrecen Kassai út 129., E-mail: pburai@envirosense.hu; [3]Photon d.o.o., Croatia, Split, Matice Hrvatske 15., E-mail: amer@teraelement.com; [4]Károly Róbert College, Faculty of Natural Resources Management and Rural Development, Institute of Agroinformatics and Rural Development, H-3500 Gyöngyös Mátrai út 36., Hungary, E-mail: lenart@karolyrobert.hu; [5]Károly Róbert College, Faculty of Natural Resources Management and Rural Development, Institute of Agroinformatics and Rural Development, H-3500 Gyöngyös Mátrai út 36., Hungary, E-mail: berke64@gmail.com; [6]University of West Hungary, Faculty of Agricultural and Food Sciences, Institute of Biosystems Engineering, H-9200, Mosonmagyaróvár, Vár 2, Hungary, E-mail: milics@mtk.nyme.hu [7]Károly Róbert College, Faculty of Natural Resources Management and Rural Development, Institute of Agroinformatics and Rural Development, H-3500 Gyöngyös Mátrai út 36., Hungary, E-mail: tomor@karolyrobert.hu; [8]Károly Róbert College, Faculty of Natural Resources Management and Rural Development, Institute of Agroinformatics and Rural Development, H-3500 Gyöngyös Mátrai út 36., Hungary, E-mail: tbiro@karolyrobert.hu

Received 10 May 2011; accepted in revised form 17 June 2011

Abstract
One of the largest industrial spills in Europe occurred in the village of Kolontár (Hungary) on October 4, 2010. The primary objective of the hyperspectral remote sensing mission was to monitor that is necessary in order to estimate the environmental damage, the precise size of the polluted area, the rating of substance concentration in the mud, and the overall condition of the flooded district as soon as possible. The secondary objective was to provide geodetic data necessary for the high-resolution visual information from the data of an additional Lidar survey, and for the coherent modeling of the event. For quick assessment and remediation purposes, it was deemed important to estimate the thickness of the red mud, particularly the areas where it was deposited in a thick layer. The results showed that some of the existing tools can be easily modified and implemented to get the most out of the available advanced remote sensing data.

Keywords: remote sensing, hyperspectral, AISA Eagle, image classification, multi sensor, industrial disaster, red mud

1. Introduction

Hungary, due to its geographical position, has unique characteristics in Europe regarding wetlands. One of the largest industrial spills in Europe occurred in the village of Kolontár (Hungary) on October 4, 2010 (Bárdossy, 2010; Ensernik, 2010; Schiermeier and Balling, 2010). Coupled with an above-average rainfall, a

large-mass of red-mud tailings (the by-product of aluminum refining) had ruptured through the retention wall of the tailings and flooded the nearby towns. The sheer mass and the complicated viscosity/flow properties of the spilled material that contained a highly alkaline solution (>12 pH) had resulted in a complex environmental disaster, requiring a multi-disciplinary approach regarding the assessment and the remediation of the situation. The research and assessment was coordinated by the Hungarian Academy of Sciences with the primary task on determining the spatial extent of the red-mud sludge spill as well as the immediate and long-term contamination effects on the environment. This study focuses on the immediate results of a comprehensive interdisciplinary survey derived from the horizontal integration of spectroscopic, the hyperspectral and thermal infrared imaging, Lidar, the heavy metal contamination of soils and the particle size distribution of red mud according to eco-toxicological, chemical and physical investigations carried out in support. A prompt response to the red mud spill made it possible to study a particular sequence of events successfully. Such studies could not have been implemented in laboratory conditions. Earlier, several studies have indicated the possibility of applying remote sensing technology in the identification of heavy metals (Ferrier, 1999; Kemper and Sommer; 2002; Choe et al. 2008); however, those contaminations had different characteristics (acidic pH) and contained different concentrations of heavy metals.

About 40 million tons of red mud is generated and stored annually worldwide, primarily by wet disposal, similar to Hungary, which represents a significant environmental and human risk and liability (Power et al. 2009). The knowledge and the procedures acquired from the Kolontár case can be successfully applied anywhere to reduce such risks in the future.

2. Materials and methods

Red mud is a product of bauxite digestion with sodium hydroxide originating from the Bayer process of alumina production. The conventional disposal is to simply pump the highly alkaline slurry into reservoirs or dykes and allow it to dry naturally (Hind et al. 1999). Red mud is composed primarily of iron oxides, quartz, sodium aluminosilicates, calcium carbonate/aluminate, titanium dioxide, and sodium hydroxide (pH 10-12). Its composition and high pH make it relatively toxic and risky to the environment (Somlai et al. 2008).

Over the years, Ajka alumina plant has generated over 30 million m^3 of red mud, ten impoundments have been constructed between the city of Ajka and Kolontár village on a relatively flat land, with the impoundment walls strengthened by a slag/ash from the nearby coal-fired power plant (Bárdossy, 2010). The flash-flood caused by the heavy rainfall of October 2010 resulted in the rupture of the north-

western wall in one of the impoundments and the subsequent evacuation of an unspecified amount of red-mud towards the town of Devecser and beyond (Fig. 1).

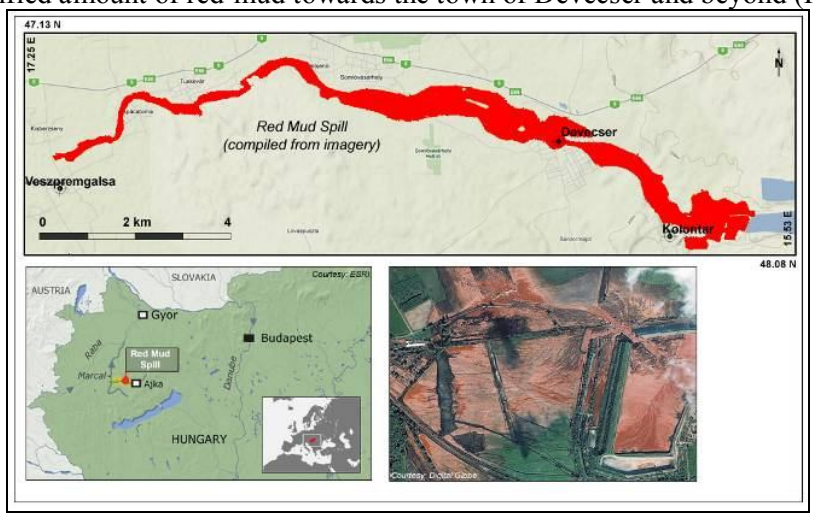

Fig. 1. Location of the area and approximate direction of red-mud spill assembled from satellite imagery (IKONOS, GeoEye).

The specialty of this event was that unique planning and implementation was necessary. Data collection with the help of remote sensing – according to the complex aims - was carried out by many experts participating in the project. Besides, data collection at the time of air-shots, the opportunity of processing different remote-sensing technologies and the collection of data corresponding both short and long term processing goals were especially considered. Table 1 shows basic data of the images gathered during our flights and air-shots.

Table 1. Main parameters of data collection

	Visible data (VIS)	**Near Infrared data (NIR)**	**Far Infrared data (FIR)**	**Hyperspectral data**	**LiDAR data**
Type of sensor	Canon 30 D	Canon 30 DIR	Hexium InfraDiagnostic System 110	AISA Eagle	Leica ALS 60
Time of flight	Oct 11, 2010 2 p.m. – 6 p.m.	Oct 11, 2010 2 p.m. – 6 p.m.	Oct 11, 2010 2 p.m. – 6 p.m.	Oct 10, 2010 11 a.m. – 2:30 p.m.	Oct 11, 2010 12 a.m. – 2 p.m.
Height of flight (AGL)	350 m, 1000 m	350 m, 1000 m	350 m, 1000 m	1655 m	800 m
Spectral range	400-700 nm	720-1150 nm	8000-14000 nm	400-970 nm (253 bands)	1064nm-
Ground resolution	0.2 m	0.2 m	0.6 m	1.1 m	4 Pts/m^2
Radiometric resolution	14/16 bit/pixel	14/16 bit/pixel	14/16 bit/pixel	14/16 bit/pixel	16 bit

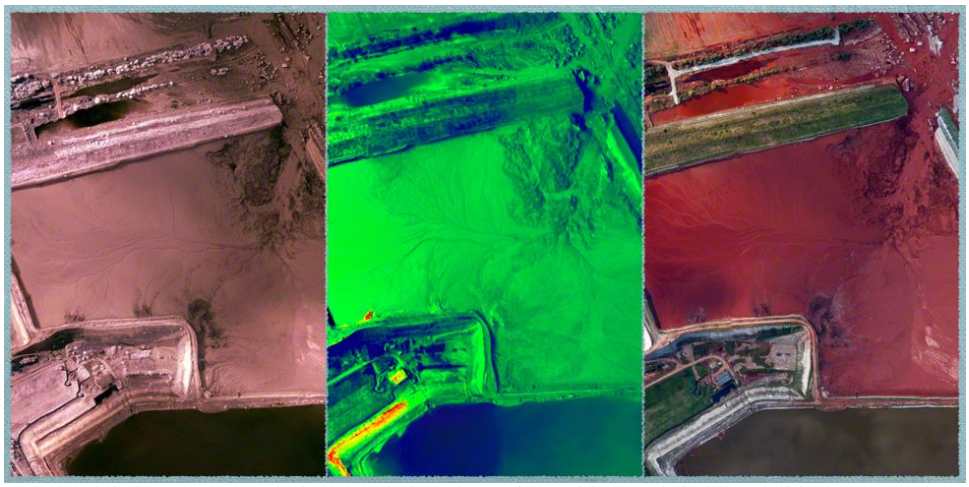

Fig. 2. High geometric resolution near infrared (a), thermal infrared (b) and visible (c) RGB pictures of the damaged reservoir.

3. Results

During the data collection five different remote sensing systems were used, and the processing of different technologies and the collected data were intended to be streamlined and combined for both short-term and long-term purposes. The approximate size of the affected area was estimated at about 1000 Ha based on the information derived from the high-resolution IKONOS satellite data (GeoEye) and airborne imagery (Disaster Management).

The high-resolution digital images taken from low flight altitude have played an important role principally in the mapping of the primary effects of the disaster and the survey of the physical condition of the reservoir. The processing and fast evaluation of the images could be carried out within a day; they were mainly used for the rapid assessment of the static state of the reservoirs. Cracks that were generated on the dam could be determined by visual interpretation, and wet areas could be defined by the analysis of thermal images.

The secondary objective was to provide geodetic data necessary for the high-resolution visual information from the data of a Lidar survey and for the coherent modeling of the event. Quantitative and qualitative information were derived from radiometrically and geometrically corrected hyperspectral images. The hyperspectral data were calibrated to reflectance using several ground-based sites exhibiting identical flat-field reflectance targets (e.g. sandy beach, calibration tarp, concrete court) throughout the area. The flat-field targets were measured with a

full-range ASD spectroradiometer, and derived spectra were used to correct airborne data applying the empirical-line method (Aspinnal et al. 2002).

In order to determine the relative abundance, concentration and dispersal of red mud and contaminated waters, SAM (Spectral Angle Mapper; Kruse et al. 1993) was initially applied to extrapolate the information of the affected area. Heavy flood had destroyed non-arboreal vegetation in the majority of the area, and red mud sediment solidified into a more-or-less homogenous layer in the field. The spectroscopic data (acquired on the ground) suggested that the water content of red mud had a strong effect on the observed reflectance values (Fig. 3).

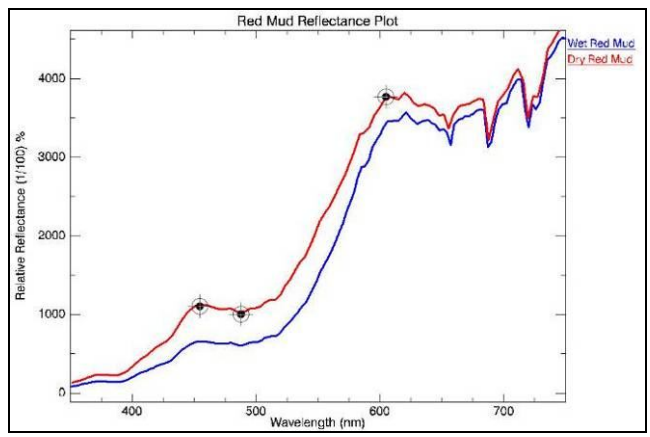

Fig. 3. Reflectance spectra of red mud

Different endmembers were used for imagery classification: dry (dry matter: 80-92 % by mass), moderately wet (dry matter: 50-80 % by mass) and wet red mud (dry matter: 15-30 % by mass) classes. To improve the classification methodology, representative soil and mud samples were measured and used as "known" endmembers for the analysis and prediction of the thickness of red mud layer (Fig. 3).

Absorption features of red mud layer were detected in the blue and green range (480-570 nm) with the reflectance maximum peak in the red region (650-720 nm). For such purpose, a Red Mud Layer Index (RMLI) was calculated from hyperspectral bands (549 nm, 682 nm) to describe the depth of red mud layer (between 0-20cm) in the affected area (Fig. 4-5).

$$RMLI = (RED_{682nm}-GREEN_{549nm})/ (RED_{682nm}+GREEN_{549nm})$$

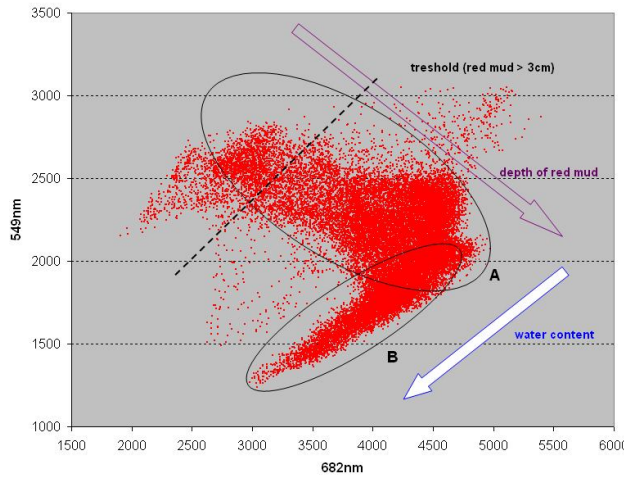

Fig. 4. Scatter plot of 549nm and 682nm wavelengths of the affected study area (28,900 pixels). Ellipse "A" represents dry and moderated wet (dry matter: 50-92%) red mud, ellipse "B" represents red mud with high wet content (dry matter less than 50%).

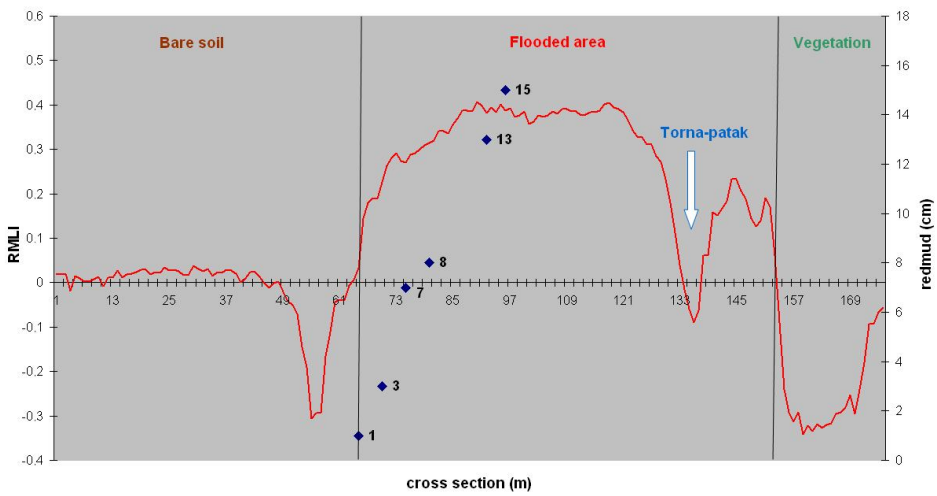

Fig. 5. Field samples (redmud thickness) and RMLI data on the examined cross-section of flooded area.(blue dots: red mud thickness (cm) of field samples, red line: RMLI)

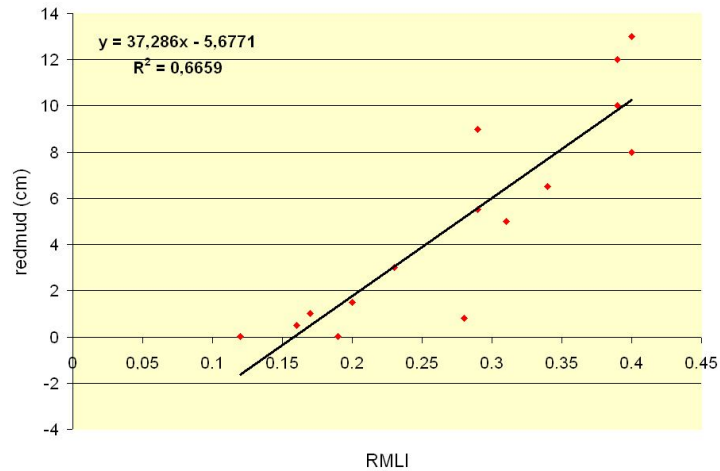

Fig. 6. Correlation between RMLI (Red Mud Layer Index), dry, and moderated wet redmud (cm) samples

Based on these parameters, for quick assessment and remediation purposes, it was considered important to estimate the thickness of the red mud, particularly in the areas where the depths of the layer were more than 3 cm (Fig. 7)

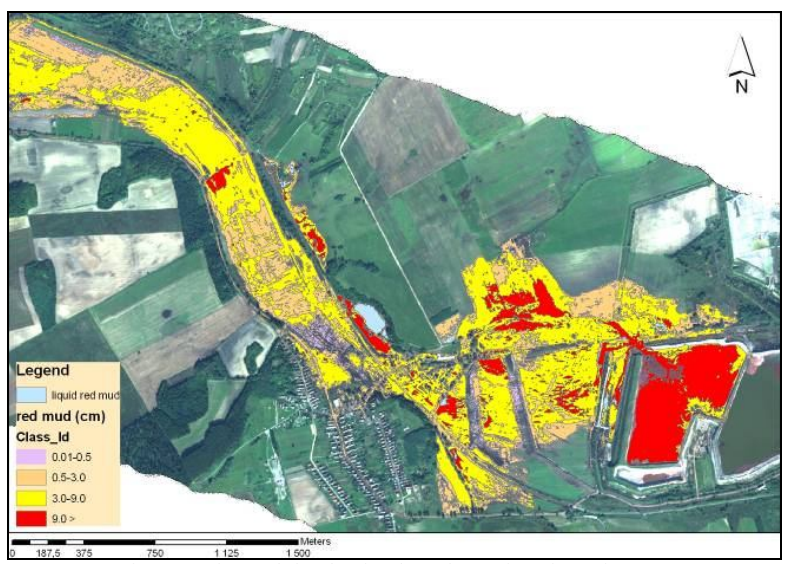

Fig. 7. Estimated depth of red mud as a function of RMLI

Flood maps, based on the primary analysis of hyperspectral images, were made within a week, while the documentation that contains detailed thematic layers was forwarded to the authorities (Disaster Management) one month after the disaster.

A digital elevation model (DEM) is the conventional data product/deliverable derived from Lidar data (Kaasalainen et al. 2005). A wetness index map (Moore at al., 1991), which is often used in pre- and post-flood analysis, is a secondary product that is often generated from a resulting DEM and mainly depends on the topographic parameters of the area (e.g. slope, structure and contributing area) of the DEM. (Lang and McCarty, 2009) In this project, the Lidar data were primarily used to create a high resolution, 3D topographic model of the ruptured reservoir wall and examine it for the possibility of continued rupture along the western and northern walls. The Lidar data were gridded to produce a high-density point-cloud that was then draped over with high resolution imagery from the Canon 3D camera and Hyperspectral imagery. The combined analysis had shown a propagation of collapse features (compromised structure) along the western retention wall and the areas have been subsequently stabilized (Fig. 8).

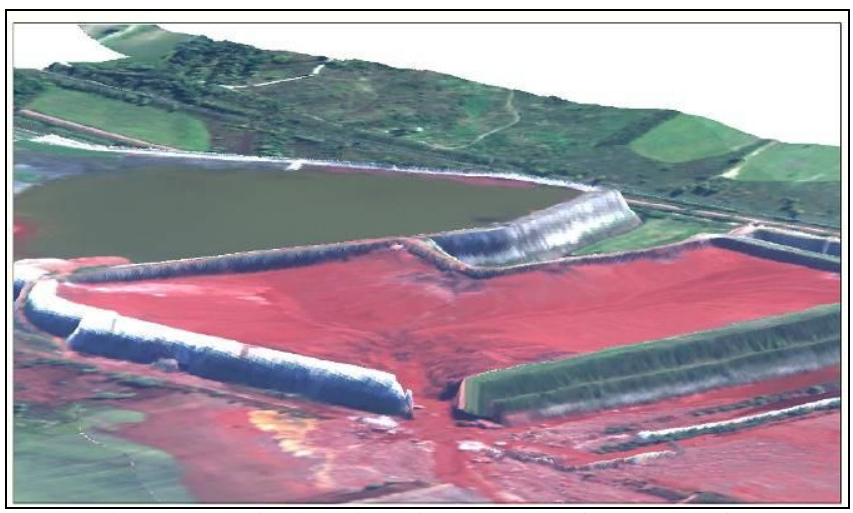

Fig. 8. Integrated Lidar and HSI data over ruptured containment dam

However, it was proposed that Lidar intensity data may be adequate for the identification of inundation even below the forest canopy, due to the strong absorption of incident near-infrared energy by water and the ability to filter the data by the order of return (Lang and McCarty, 2009). Even though majority of the water had already receded, in places the red mud was still sufficiently wet to attempt this approach on the basis of energy attenuation from a wet and dull surface. The Lidar intensity data were treated as a “traditional geophysical” dataset (e.g. similar to magnetic or gamma-ray data), with X-Y-Z coordinates plus extrapolated intensity data assigned to the particular point(s), filtered to attenuate some of the noise (e.g. Gaussian filter), and then gridded (Nearest Neighbour) to produce a relative intensity map. It was shown that the heavy deciduous vegetation in some places had given false-positive results by attenuating the signal, while in

the relative clear locations it was possible to distinguish the red-mud flooded areas from unaffected areas or at least the areas where the red-mud was still relatively wet at the time of the data collection, which facilitated the neutralization and the effort of the cleaning (Fig. 8).

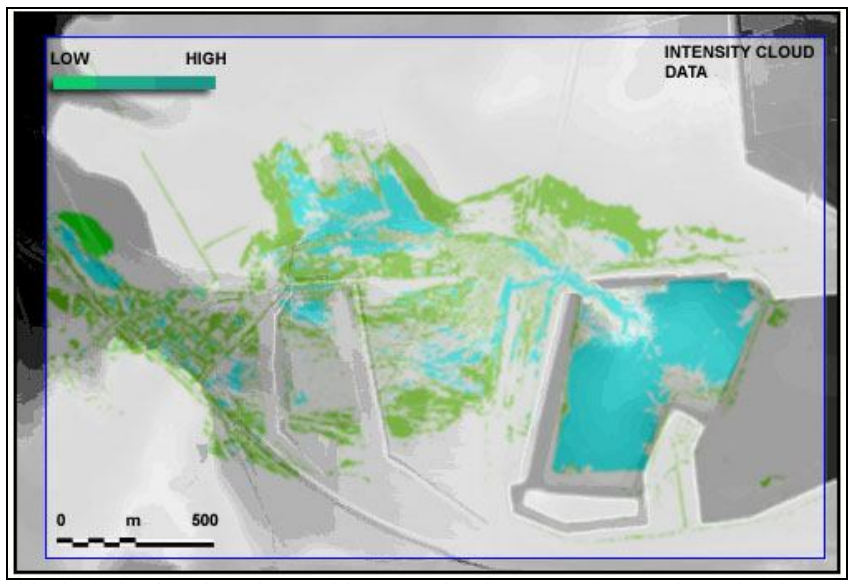

Fig. 9. Lidar intensity data draped over Lidar DTM showing areas of return absorption due to wet mud.

4. Discussion

This report on the quick assessment of the caustic red mud spill shows that some of the existing tools can be readily modified and implemented to get the most out of the available remote sensing data. A combination of various imagers can complement each other, take particular advantages and reduce their individual shortcomings in an emergency-response situation. The results suggest that even in quick response, it was possible to obtain and pass on the obtained information quickly using relatively simple processing and evaluation methods.

Although, the primary evaluation of hyperspectral images occurred within a week, the quick and accurate evaluation of pollutions that affect similarly large areas would require such robust systems that are appropriate for the quick and accurate solution of the problem by the use of different classification algorithms. Fortunately, examples for many practical applications can be found in the development of the processing of hyperspectral images, either for the assessment of red mud flooded areas (Bakos et al. 2011; Kugler, 2011), which can be used

effectively in the future, if a rapid assessment of a similar emergency incident would be necessary.

Furthermore, hyperspectral acquisitions were extended over the flooded area in order to record the state of vegetation and soil. This database can be used for change detection such as vegetation stress and dusting.

Acknowledgement

We say a special thank to Károly Róbert College for the financial support of the aerial survey. Furthermore, special thanks to the Envirosense Hungary Ltd., Hexium Ltd., Photon d.o.o. Split, and BlomInfo companies,who participated in the data processing work, and for the contributors involved in the field work from the Geological Institute of Hungary, University of West Hungary, Hungarian Institute of Agricultural Engineering, and University of Debrecen. The scientific coordination of the work was conducted by the expert group of the Hungarian Academy of Sciences and the National Disaster Management.

References

Aspinall, R.J. – Marcus, W.A. – Boardman, J.W. (2002): Considerations in collecting, processing, and analyzing high spatial resolution hyperspectral data for environmental investigations. *Journal Geographical Syst*em **4**: 15-29.

Bakos, K. – Gamba, P. – Burai, P. (2011): Rapid estimation of point source chemical pollutant coverage in catastrophe situation using hierarchical binary decision tree ensemble end probability membership value based ensemble approaches. 3rd IEEE GRSS Workshop on Hyperspectral Image and Signal Processing-WHISPERS 2011, Lisboa, Portugal, 2011. In press.

Bárdossy, G., (2010): Red mud catastrophe in Hungary. *IAMG Newsletter*. **81**: 5.

Chi, M. – Feng, R. – Bruzzone, L. (2008): Classification of hyperspectral remote-sensing data with primal SVM for small-sized training dataset problem. *Advance in Space Research* **41** (11): 1793-1799.

Choe, E. – Meer, F. – Ruitenbeek, F. – Werff, H. – Smeth, B. – Kim, K.W. (2008): Mapping of heavy metal pollution in stream sediments using combined geochemistry, field spectroscopy, and hyper spectral remote sensing: a case study of the Rodalquilar mining area. *Remote Sensing of Environment* **112**: 3222-3233.

Enserink, M. (2010): After red mud flood, scientists try to halt wave of fear and rumors. *Science* **330**: 432-433.

Ferrier, G. (1999): Application of imaging spectrometer data in identifying environmental pollution caused by mining at Rodaquilar, Spain. *Remote Sensing of Environment*, **68**: 125-137.

Hind, A.R. – Bhargava. S.K. – Grocott. S.C. (1999): The surface chemistry of Bayer process solids: a review. Colloids Surf. A: Physicochem. Eng. Aspects. **146**: 359-374.

Kaasalainen, S. – Ahokas, E. – Hyyppa, J. – Suomalainen, J. (2005): Study of surface brightness from backscattered laser intensity: calibration of laser data. *IEEE Geoscience and Remote Sensing Letters* **2**: 255-259.

Kemper, T. – Sommer, S. (2002): Estimate of heavy metal contamination in soils after a mining accident using reflectance spectroscopy. *Environmental Science and Technology* **36**: 2742-2747.

Kruse F. A. – Lefkoff A.B. – Boardman J. B. – Heidebrecht K.B. – Shapiro A.T. – Barloon P.J. – Goetz, A.F.H. (1993): "The Spectral Image Processing System (SIPS) - Interactive Visualization and Analysis of Imaging spectrometer Data". *Remote Sensing of the Environment* **44**: 145-163.

Kugler, Zs. (2011) The red sludge spill crisis from satellite images near Ajka / Hungary. *Geodézia és Kartográfia* **63**: 20-23. (In Hungarian)

Lang, M.W. – McCarty, G.W. (2009): Lidar intensity for improved detection of inundation below the forest canopy. *Wetlands*, **29**: 1166–117.

Moore, I.D. – Grayson, R.B. – Ladson. A.R. (1991): Digital terrain modelling: a review of hydrological, geomorphological, and biological applications. *Hydrological Processes* **5**: 3-30.

Power, G. – Gräfe, M. – Klauber, C. (2009): Review of current bauxite residue management, disposal and storage: practices, engineering and science. CSIRO Document DMR-3608

Schiermeier, Q. – Balling, Y. (2010): Analysis lags on Hungarian sludge leak. *Nature* doi:10.1038/news.2010.531

Somlai, J. – Jobbágy, V. – Kovács, J. – Tarján, S. – Kovács, T. (2008): Radiological aspects of the usability of red mud as building material additive. *J. Hazard. Materials* **150**: 541-545.